Supplementary Information

S1. Oxidation level of pristine SiO_x

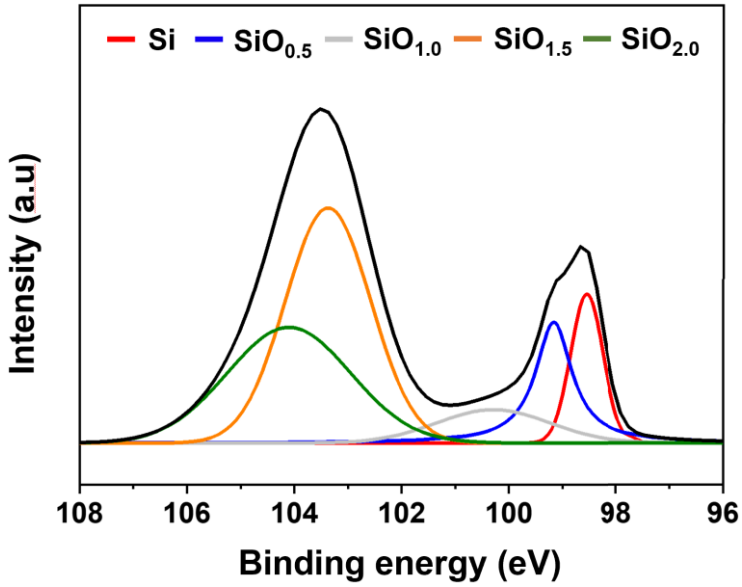

Figure S1. The Si2p binding energy spectrum of pristine SiO_x sample.

The oxidation level of pristine SiO_x sample was investigated using X-ray photoelectron spectroscopy (XPS) measurement. **Figure S1** shows the Si2p binding energy spectrum of pristine SiO_x sample. The Si2p bands are divided into five lower bands that determine the oxidation levels: Si (98 eV), $SiO_{0.5}$ (98.7 eV), $SiO_{1.0}$ (100 eV), $SiO_{1.5}$ (103.5 eV), and SiO_2 (104.1 eV). The x value (oxidation level) of SiO_x is calculated using the following equation.[1,2]

$$x = \frac{(0 \times a) + (0.5 \times b) + (1 \times c) + (1.5 \times d) + (2 \times e)}{a + b + c + d + e}$$

Herein, x is the valence state of Si in SiOx, and a, b, c, d, and e denote the binding strengths of Si, $SiO_{0.5}$, $SiO_{1.0}$, $SiO_{1.5}$, and SiO_2 in Si2p, respectively. As a result of calculating the degree of oxidation using the above equation, it was found that the x value of the SiO_x used in this work was 1.04.

References

1. Alfonsetti, R.; Lozzi, L.; Passacantando, M.; Picozzi, P.; Santucci, S. XPS studies on SiOx thin films, *Appl. Surf. Sci.* **1993**, *28*, 137-151.
2. Sublemontier, O.; Nicolas, C.; Aureau, D.; Patanen, M.; Kintz, H.; Liu, X.; Gaveau, M.A.; Garrec, J.L.L.; Robert, E.; Barreda, F.A.; Etcheberry, A.; Reynaude, C.; Mitchell, J.B.; Miron, C. X-ray photoelectron spectroscopy of isolated nanoparticles, *J. Phys. Chem. Lett.* **2014**, *5*, 3399.

S2. TGA analysis of pitch

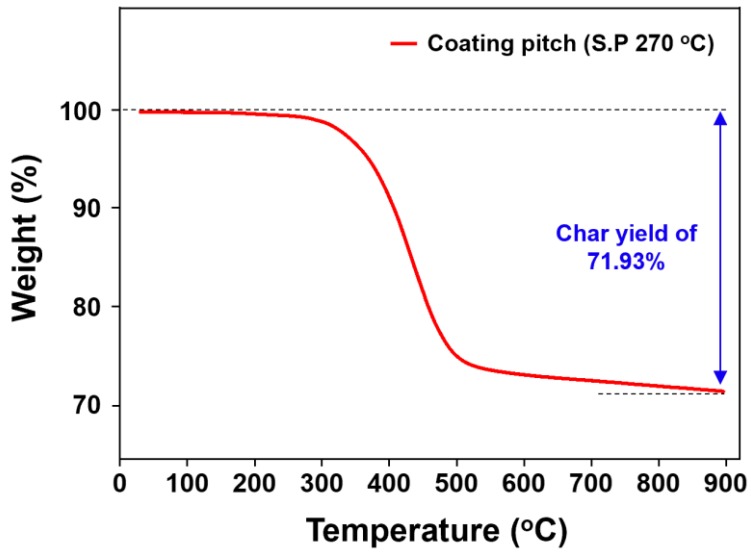

Figure S2. Thermogravimetric analysis (TGA) curve of the pitch.

S3. sp^2/sp^3 carbon ratio in SiO_x@C composite

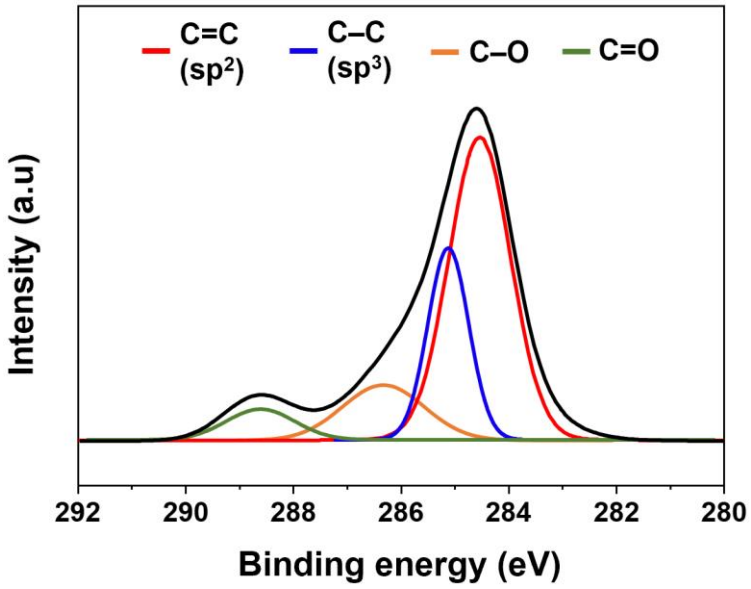

Figure S3. Deconvolution of the C1s XPS spectrum of the SiO_x@C_8:2 composite.

Table S1. Assignment of C1s XPS peaks taken from the SiOx@C_8:2 composite.

Binding energy (eV)	Peak Area (%)	Assignment
284.5	56.7	C=C (sp^2)
285.1	25.1	C–C (sp^3)
286.8	10.3	C–O
288.4	7.9	C=O

The sp^2/sp^3 bonding ratio of the carbon layer in the SiO_x@C composite was investigated. **Figure S3** shows the C1s XPS peak taken from the SiO_x@C_8:2 composite. The XPS spectrum was background-subtracted and then deconvoluted. C1s peaks in the XPS spectrum are commonly used to identify chemical states and orbital type of the amorphous carbon. The C1s spectrum of the SiO_x@C_8:2 composite was deconvoluted into four sub-peaks with the positions at 284.5, 285.1, 286.8 and 288.4 eV, respectively. The assignments of the C1s peaks are given in **Table S1**. The C1s peaks around 284.5 and 285.1 eV corresponds to the graphitic structure (sp^2) and the diamond structure (sp^3), respectively.[1] From the **Figure S3**, it is obvious that the carbon layer in the SiO_x@C composite exists in the sp^2 configuration more than the sp^3 configuration, and it is revealed that the sp^2/sp^3 ratio is about 2.26.

References

1. Morgan, D.J. Comments on the XPS analysis of carbon materials, *C* **2021**, *7*, 51.

S4. EIS analysis

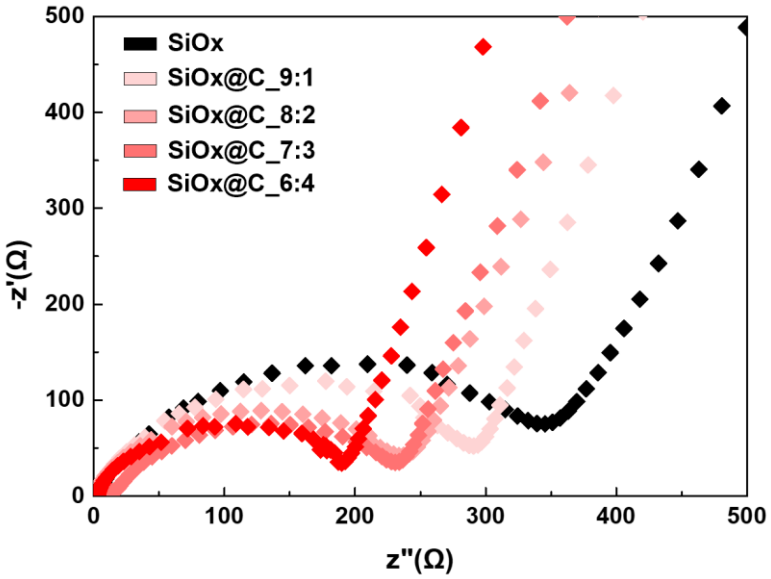

Figure S4. Nyquist plots of the pristine SiO_x, SiO_x@C_9:1, SiO_x@C_8:2, SiO_x@C_7:3, and SiO_x@C_6:4 composite samples.

S5. Discharge capacity of carbon layer

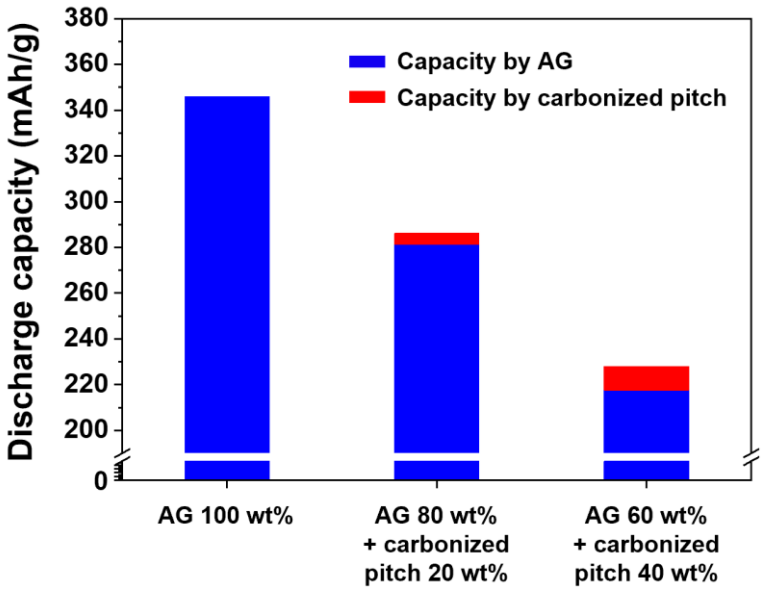

Figure S5. Comparison of the discharge capacity of the anodes prepared with AG and AG+carbonized pitch (20 wt%, 40 wt%).

Table S2. Comparison of discharge capacity by anode active material components.

Active material	Measured discharge capacity (A)	Discharge capacity by components	
		AG [a] (B)	carbonized pitch (A–B)
AG 100 wt%	345.8 mAh/g	345.8 mAh/g	0 mAh/g
AG 80 wt% + carbonized pitch 20 wt%	281.3 mAh/g	276.6 mAh/g	4.7 mAh/g
AG 60 wt% + carbonized pitch 40 wt%	217.7 mAh/g	207.5 mAh/g	10.2 mAh/g

[a] The discharge capacity of AG in the composite was calculated according to the content ratio based on 100 wt% AG.

Control experiments were carried out by using carbonized pitch as a comparison material to confirm the capacity contribution of the carbon layer in the SiO_x@C composite. **Figure S5** shows the discharge capacity of the anode prepared with artificial graphite (AG) and samples with carbonized pitch added to AG at 20 wt% and 40 wt%, respectively. The theoretical capacity of AG (MAGE, < 25 μm, Hitachi, Japan) used as an active material is 350 mAh/g, and the actual measured value was 345 mAh/g at 0.1 C after three stabilization cycles at a rate of 0.1 C. In the case of samples containing 20 and 40 wt% of carbonized pitch compared to AG,

the discharge capacities were measured at 281.3 mAh/g and 217.7 mAh/g, respectively. The discharge capacity of the carbonized pitch could be indirectly inferred from the actual measured discharge capacity by subtracting the theoretical capacity of 80 and 60% of AG (**Table S2**). Based on these results, the carbonized pitch is expected to have a capacity of approximately 25 mAh/g, and the carbon layer of the SiO_x@C composite is believed to not contribute significantly to the capacity.

S6. Charge storage mechanism

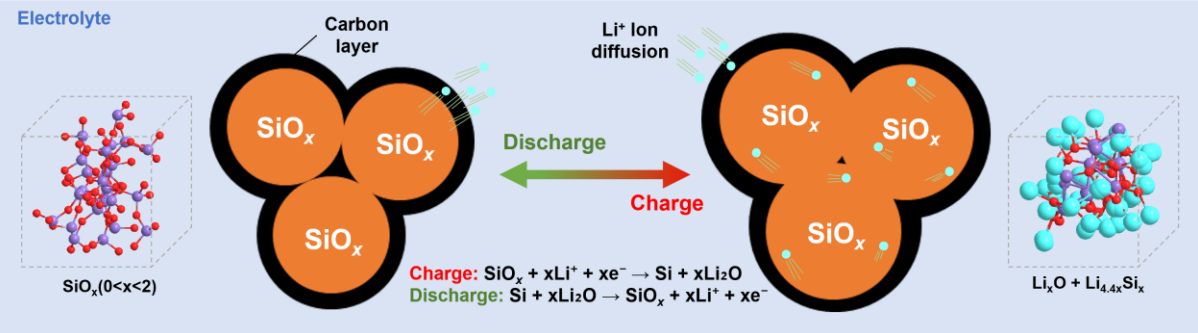

Figure S6. Schematic of charge storage mechanism of SiO_x@C composite.

The charge storage mechanism according to lithiation/delithiation process of SiOx@C composite was modeled (**Figure S6**). The charge storage mechanism of SiO_x@C composite is mainly based on the chemical reaction between SiO_x and lithium ions. SiO_x absorbs and releases lithium ions during charging/discharging process. The detailed chemical reaction can be expressed as:

Charge : $SiO_x + xLi^+ + xe^- \rightarrow Si + xLi_2O$ / Discharge : $Si + xLi_2O \rightarrow SiO_x + xLi^+ + xe^-$

Unlike SiO_x, the carbon layer of SiO_x@C composite is not directly involved in charge storage. In general, amorphous carbon is known to have a small contribution to securing discharge capacity. It is believed that the amorphous carbon layer introduced on the SiO_x surface will store lithium ions only in local voids created due to the unstable stacked structure of the carbon layer. On the other hand, this carbon layer plays a crucial role in buffering the volume expansion of SiO_x during lithiation/delithiation processes, enhancing electrical conductivity, and preventing direct contact with the electrolyte.

S7. Compilation of different investigations using various silicon oxide@carbon composites

Table S3. Electrochemical performance of various silicon oxide@carbon composites.

Active material	ICE	Discharge capacity	Capacity retention	Ref.
SiO_x@C	90.7%	1,022 mAh g^{-1}	53.5%	[1]
SiO_x@C	66.7%	674 mAh g^{-1}	83.5%	[2]
SiO_x@C	47.3%	800 mAh g^{-1}	36%	[3]
SiO_x@C	66.1%	999 mAh g^{-1}	85.5%	[4]
SiO_x@C	46.7%	600 mAh g^{-1}	97%	[5]
SiO_x@C	59%	888 mAh g^{-1}	60.7%	[6]
SiO_2@graphite	66%	433 mAh g^{-1}	60.9%	[7]
SiO_x@C	74.9%	685.8 mAh g^{-1}	65.4%	This work

A compilation of LIBs performance investigations using silicon oxide-based anode materials is presented in **Table S3**. It shows the electrochemical properties (ICE, discharge capacity and capacity retention rate) by various silicon oxide@carbon composites as reported in the literature. The battery performance stongly depends on several parameters, such as type of anode components (conductive additives, binder and electrolyte), testing condition (potential or charge and discharge current), operating condition (temperature and humidity), *etc*. Therefore, it is not appropriate to directly compare the results under different test conditions, and it can only be inferred from relative values by comparing them. In this work, the SiO_x@C_8:2 exhibited ICE 74.9%, discharge capacity 685.8 mAh g-1 and capacity retention 65.4%, which is similar or much larger than those of reported silicon oxide@carbon-based materials (**Table S3**).

References

1. Jiang, F.; Sun, Y.; Zhang, K.; Liu, Y.; Feng, X.; Xiang, H. SiO_x/C anodes with high initial coulombic efficiency through the synergy effect of pre-lithiation and fluoroethylene carbonate for lithium-ion batteries, *Electrochim. Acta* **2021**, *398*, 139315.
2. Wu, W.; Shi, J.; Liang, Y.; Liu, F.; Peng, Y.; Yang, H. A low-cost and advanced SiO_x–C composite with hierarchical structure as an anode material for lithium-ion batteries, *Phys. Chem. Chem. Phys.* **2015**, *17*, 13451-13456.
3. Wang, J.; Zhao, H.; He, J.; Wang, C.; Wang, J. Nano-sized SiO_x/C composite anode for lithium ion batteries, *J. Power Sources* **2011**, *196*, 4811-4815.
4. Liu, Z.; Guan, D.; Yu, Q.; Xu, L.; Zhuang, Z.; Zhu, T.; Zhao, D.; Zhou, L.; Mai, L.

Monodisperse and homogeneous SiO_x/C microspheres: a promising high-capacity and durable anode material for lithium-ion batteries, *Energy Storage Mater.* **2018**, *13*, 112-118.
5. Ju, Y.; Tang, J.A.; Zhu, K.; Meng, Y.; Wang, C.; Chen, G.; Wei, Y.; Gao, Y. SiO_x/C composite from rice husks as an anode material for lithium-ion batteries, *Electrochim. Acta* **2016**, *191*, 411-416.
6. Xia, H.; Yin, Z.; Zheng, F.; Zhang, Y. Facile synthesis of SiO_2/C composites as anode materials for lithium-ion batteries, *Mater. Lett.* **2017**, *205*, 83-86.
7. Zhang, L.; Shen, K.; He, W.; Liu, Y.; Guo, S. SiO_2@ graphite composite generated from sewage sludge as an anode material for lithium-ion batteries, *Int. J. Electrochem. Sci.* **2017**, *12*, 10221-10229.